

## Spin-resolved photoemission study of the reaction of O<sub>2</sub> with fcc Co(100)

W. Clemens and E. Vescovo

*Institut für Festkörperforschung, Forschungszentrum Jülich, D-5170 Jülich, Germany*

T. Kachel

*Berliner Elektronenspeicherring-Gesellschaft für Synchrotronstrahlung m.b.H. (BESSY), Lentzeallee 100, D-1000 Berlin 33, Germany*

C. Carbone and W. Eberhardt

*Institut für Festkörperforschung, Forschungszentrum Jülich, D-5170 Jülich, Germany*

(Received 24 February 1992)

The effect of O<sub>2</sub> chemisorption on the electronic structure and magnetism of fcc Co overlayers, grown epitaxially on Cu(100), has been studied by use of spin- and angle-resolved photoelectron spectroscopy. At room temperature, for exposures between 2 and 7 L of O<sub>2</sub>, oxygen adsorbs dissociatively in an ordered  $c(2\times 2)$  structure. [1 langmuir (L)  $\equiv 10^{-6}$  Torr sec.] The chemical interaction between the adsorbate and the substrate manifests itself through a reduction of the 3d surface-state emission at  $\Gamma$  near  $E_F$ . The oxygen bands exhibit an induced exchange splitting of  $0.2\pm 0.1$  eV at the center of the surface Brillouin zone. With higher O<sub>2</sub> exposure, corresponding to the formation of a CoO surface phase, the photoemission spectra show evidence for strong correlation effects in the electronic structure. A satellite appears about 10 eV below  $E_F$  in the spectra. The formation of the CoO surface-oxide phase is accompanied by a decrease in the photoelectron spin polarization revealing the quenching of the surface ferromagnetic order. At low temperatures (150 K) and high exposures of O<sub>2</sub> the formation of a Co<sub>3</sub>O<sub>4</sub> phase was observed, which again has a different electronic structure.

### I. INTRODUCTION

New perspectives have been opened in the study of the interaction of O<sub>2</sub> with 3d transition-metal surfaces by recent developments in metal epitaxy. Nonequilibrium phases of the 3d transition metals now become accessible to experimental investigation. Single crystals of fcc Fe, fcc and bcc Co, and bcc Ni are stable at room temperature in the form of ultrathin overlayers.<sup>1</sup> The study of these materials will provide more insight into the interplay between electronic and atomic structure and the correlation of these properties with the magnetic and chemisorption behavior of these materials.

Here we present a spin- and angle-resolved photoemission study of the chemical reaction of O<sub>2</sub> with the fcc Co(100) surface. A specific goal of this study is the investigation of the effects of oxidation on the surface magnetism of metallic Co.

Fe and Ni surface oxidation have been rather extensively investigated.<sup>2</sup> Models of these interactions have included the possible formation of magnetic dead layers as well as the presence of magnetic moments on the adsorbate. In the more recent oxidation studies, indications of the presence of an induced magnetic moment on the adsorbate prevail over those of the presence of magnetically dead layers. The O-2p-derived bands of chemisorbed oxygen on Ni(110),<sup>3</sup> on Fe(110),<sup>4</sup> and on Fe(100) (Ref. 5) are found to exhibit an exchange splitting. Huang and Hermanson<sup>6</sup> predicted in a theoretical study the presence of a magnetic moment in oxygen chemisorbed on Fe(100).

Nevertheless, the question about the influence of chemisorption on surface magnetism is not yet unambiguously clarified. In particular, no information on single-crystalline Co is presently available.

Bulk Co is stable at room temperature in the hcp form. The preparation of a well-ordered and atomically clean single-crystal surface of the hcp phase is hindered by the hcp-fcc phase transition at 720 K. Cleaning procedures require repeated cycles through the phase transition temperature.<sup>7</sup> The oxidation studies of Co single crystals have therefore been restricted to investigations on recrystallized samples of a rather limited crystalline quality. Castro and Küppers<sup>8</sup> and Matsuyama and Ignatiev<sup>9</sup> report a first absorption stage for low-oxygen exposures on hcp Co followed by the formation of an oxide phase at higher exposures. Maglietta *et al.*<sup>10</sup> found that the interaction of the fcc (100) surface with oxygen produced ordered chemisorbed layers with first a  $p(2\times 2)$  and then a  $c(2\times 2)$  reconstruction. They conclude from a low-energy electron-diffraction (LEED) analysis that oxygen in the  $c(2\times 2)$  reconstruction is chemisorbed in the four-fold hollow sites formed by four adjacent substrate atoms. The distance of the chemisorbed oxygen layer to the Co surface is found to be 0.8 Å. The O-Co atomic distance (1.94 Å) is smaller than in CoO (2.12 Å). The atomic arrangement and metal-oxygen distances are analogous to those found in Ni(100)  $c(2\times 2)$ -O.<sup>11</sup> There is only one study on the oxidation of thin epitaxial Co films,<sup>12</sup> but without analysis of the changes in surface magnetism.

## II. EXPERIMENT

We have prepared fcc Co overlayers by epitaxial growth, *in situ*, on Cu(100) surfaces. The growth of Co on Cu(100) has been extensively studied.<sup>12–16</sup> Co grows in the fcc phase up to 20 monolayers (ML) with a small tetragonal distortion.<sup>13</sup> Co layers thicker than 2 ML are ferromagnetically ordered at room temperature with the easy magnetization axis along the in-plane  $\langle 110 \rangle$  direction.

We have studied the oxidation of Co layers by spin- and angle-resolved photoemission, with a 100-keV Mott polarimeter for spin analysis.<sup>17</sup> As a light source we used synchrotron radiation from the TGM5 Undulator beamline at the Berliner Elektronenspeicherring-Gesellschaft für Synchrotronstrahlung m.b.h. (BESSY) storage ring.<sup>18</sup> The study has been complemented by Auger and LEED analysis. We present here the results of the oxidation of relatively thick fcc Co films (10–15 ML) that have already developed a bulklike electronic structure.<sup>19</sup>

## III. RESULTS AND DISCUSSION

### A. Spin-integrated valence-band photoemission spectra: Auger and LEED analysis

We have studied the oxidation process at room temperature and at low temperature (150 K). First we want to discuss the results obtained at room temperature. Spin-integrated photoemission spectra measured for increasing oxygen exposures at room temperature are shown in Fig. 1. The spectra are recorded with 45-eV photon energy in

normal electron emission. The clean Co spectrum shows 3*d* emission in the region within 3 eV from the Fermi level. Most of these features originate from the spin-up and spin-down states with bulklike character near the  $\Gamma$  symmetry point, as discussed earlier.<sup>19</sup> A small shoulder near 3.5 eV is due to the Cu substrate emission. Exposing the clean Co surface to O<sub>2</sub> produces drastic changes in the spectra.

We distinguish in the following between two distinct stages of the oxygen reaction with fcc Co. Oxygen exposures up to 6 L correspond to the first stage [1 langmuir (L)  $\equiv 10^{-6}$  Torr sec]. In this range of exposures the photoemission spectra (see Fig. 1) show the growth of an oxygen-induced electronic state near 6-eV binding energy. For exposures above 2 L the LEED pattern has  $c(2 \times 2)$  symmetry. The intensity and sharpness of the LEED spots reach a maximum at 5–6 L, followed by a rapid decrease at higher exposures, in qualitative agreement with the results of Maglietta *et al.*<sup>10</sup>

This low-exposure regime corresponds to the formation of an ordered dissociative adsorption stage, where the oxygen atoms are chemisorbed in the  $c(2 \times 2)$  symmetry.<sup>10</sup> In this stage the photoemission spectra show also some changes induced by the oxygen adsorption on the Co 3*d* valence states. The most remarkable effect is the attenuation of the peak near the Fermi level. Our previous study of the electronic band structure of clean Co layers has identified a two-dimensional spin-up surface state (or surface resonance) at 0.6-eV binding energy. The strong changes of the intensity near  $E_F$  with low oxygen exposure confirms the surface origin of this feature.

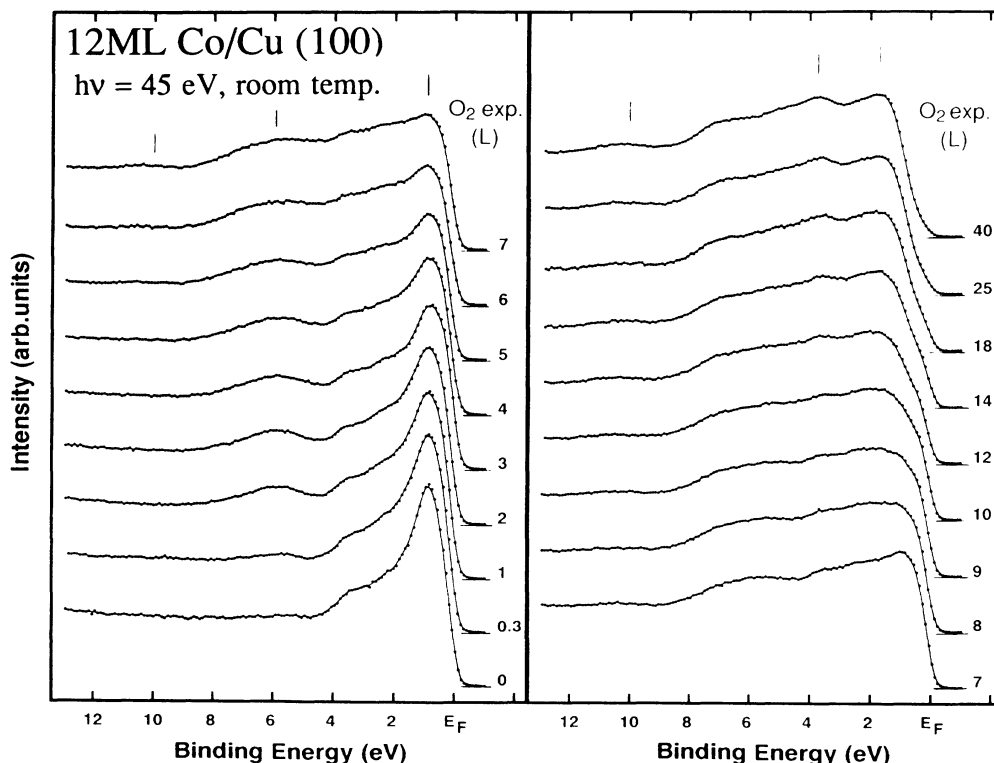


FIG. 1. Spin-integrated energy distribution curves of (12 ML Co)/Cu(100) taken in normal emission with *s*-polarized light of 45-eV photon energy. The spectra for different oxygen exposures at room temperature ( $T = 300$  K) are shown.

Further evidence will be provided in the following by the spin-resolved spectra.

In the second oxidation stage, above 7 L exposure, several additional features appear in the photoemission spectra. These changes are correlated to the disappearance of the ordered  $c(2 \times 2)$  reconstruction observed by LEED. Near 10-eV binding energy a satellite appears in the photoemission spectra with intensity increasing with oxygen exposure. In the 4–8-eV binding-energy region a broad feature develops, which clearly includes several components. Also, the Co 3*d* valence-band emission changes its shape dramatically. Additional Co-3*d*-derived features grow at 1.9-eV and 3.8-eV binding energy. The development of the spectra described above takes place mostly between 7 and 21 L oxygen exposure. For higher exposures only small changes are observed, indicating that a saturation limit is being approached.

We identified the second oxygen reaction stage as the formation of a surface oxide phase. This identification seems unambiguous if the spectra obtained for high exposures are compared to those of the bulk monoxide, CoO.<sup>20</sup> Figure 2 shows that all the spectral features have the same binding energy and a very similar overall shape in the two systems. We conclude that the photoemission spectra allow one to identify the product of the surface reaction as a surface CoO.<sup>20</sup> We therefore identify the feature growing with the oxidation at a binding energy of about 10 eV in the spectra as a correlation satellite arising from the enhanced localization of the 3*d* electrons.<sup>21</sup>

To obtain a better understanding of the oxidation process we have also characterized the sample by Auger electron spectroscopy. Figure 3 shows the measured AES oxygen *KLL* (503 eV) to cobalt *LMM* (775 eV) peak-to-peak ratio as a function of oxygen exposure. Here one can also identify two distinct reaction stages. First, the sticking coefficient is high and the Auger ratio increases drastically up to about 2 L oxygen exposure. Then a plateau at  $R \approx 0.3$  is observed for exposures up to 6 L with a low sticking probability, indicating the formation of the  $c(2 \times 2)$  adsorption stage (I). Above  $\approx 6$  L exposure there is again a drastic increase of the sticking coefficient and, thus, of the Auger ratio; this is the onset of the second stage (II), reaching a saturation limit of  $O/Co \approx 1.5$ . An equal concentration of Co and O in the sample corresponds to an Auger intensity ratio of  $I(O)/I(Co) \approx 1.9$ .<sup>9</sup> Our interpretation of this result is that within the surface layers the concentration of Co and O is close to 1:1, corresponding to the formation of CoO, while some of the Co layers underneath (within the probing depth) have still not reacted. An analogous behavior of the Auger ratio has been detected by Matsuyama and Ignatiev,<sup>9</sup> who have studied the oxidation of the hcp (0001) Co surface.

The results obtained by exposing the Co surface to oxygen at a low temperature (150 K) are shown in Fig. 4. These spectra are, in many aspects, similar to those presented in Fig. 1, especially for exposures up to 5 L. Additional features appear in the spectra for oxygen exposures above 5 L. We attribute these changes again to a second reaction stage with formation of a surface-oxide phase. The comparison [in Fig. 2(b)] with the bulk oxide

spectra indicates that the surface-oxide phase formed at low temperature corresponds at least partially to bulk  $Co_3O_4$ .

### B. Spin-resolved valence-band photoemission spectra

Figure 5 shows spin-resolved-spectra taken in normal emission with 45-eV photon energy and oxygen exposures at room temperature up to 10 L. The filled triangles ( $\blacktriangle$ ) correspond to emissions from majority-spin electrons and the open circles ( $\circ$ ) to that from minority-spin electrons. The peak at 0.9-eV binding energy in the minority-spin spectrum of the clean sample (the bottommost spectrum in Fig. 5) is due to emission from the  $\Delta_5(\downarrow)$  band near the  $\Gamma$ -symmetry point. The structure in the majority-spin spectrum is broader because it contains two contributions, the emission of the  $\Delta_5(\uparrow)$  state (near  $\Gamma$ ) at about 2.4-eV binding energy and another peak near the Fermi

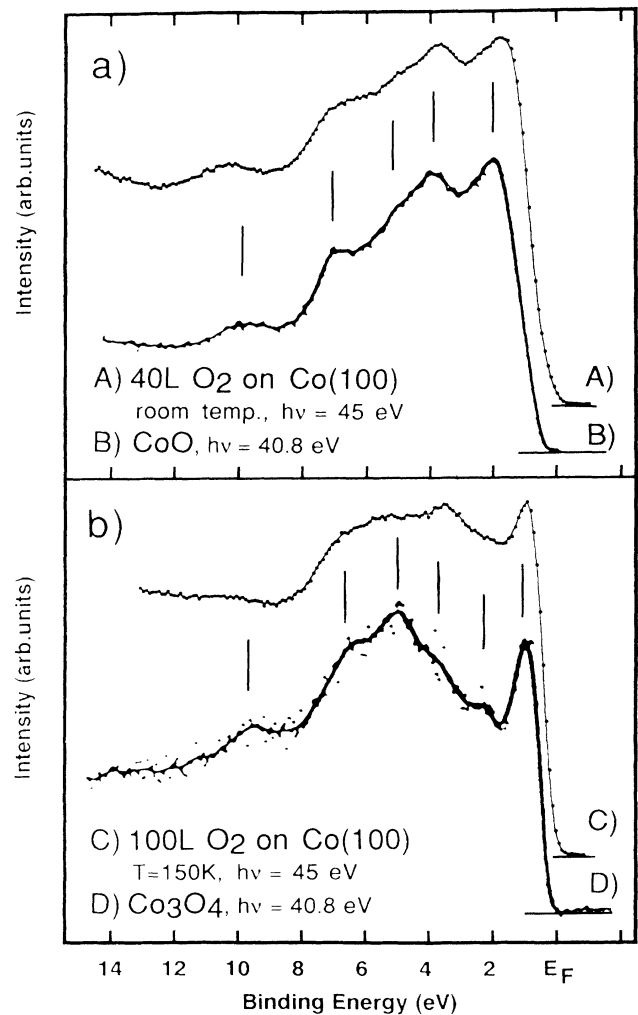


FIG. 2. Comparison of photoemission spectra with saturated oxygen exposure on (14 ML Co)/Cu(100) with bulk CoO and  $Co_3O_4$  spectra of Ref. 20: (a) spectrum with oxygen exposure at room temperature compared with a bulk CoO spectrum; (b) spectrum with oxygen exposure at  $T = 150$  K compared with a bulk  $Co_3O_4$  spectrum.

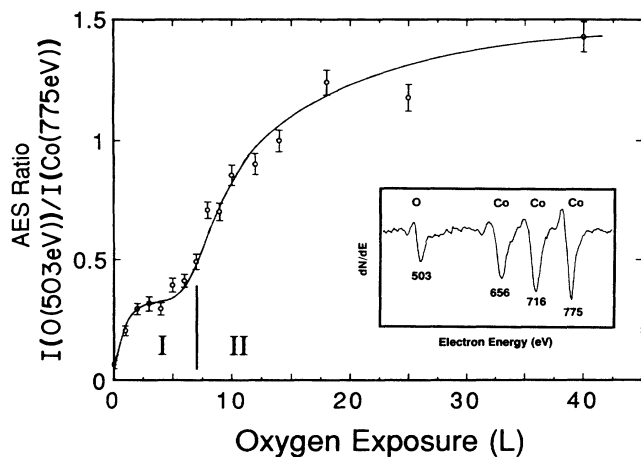


FIG. 3. Auger analysis of the adsorption process of  $O_2$  on (14 ML Co)/Cu(100) at room temperature. Ratio of the Auger peak-to-peak intensity of oxygen (503 eV) and cobalt (775 eV) vs oxygen exposure. I and II indicate the regions of formation of two different oxidation stages. Inset: derivative the Auger spectrum after 6 L  $O_2$  exposure.

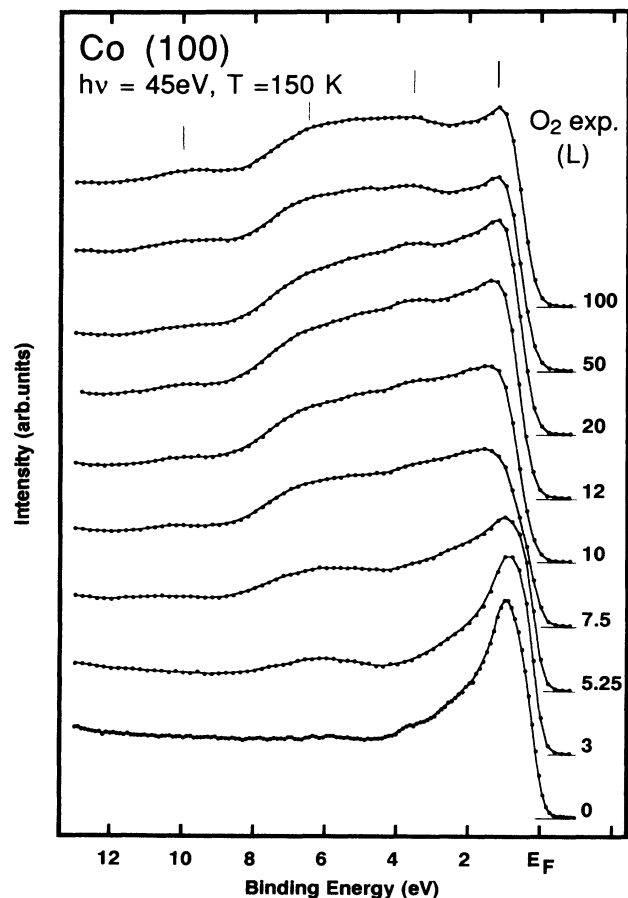


FIG. 4. Spin-integrated energy distribution curves of (14 ML Co)/Cu(100) taken in normal emission with *s*-polarized light of 45-eV photon energy. The spectra for different oxygen exposures at  $T = 150$  K are shown.

energy that has been assigned to a surface state or resonance.<sup>19</sup>

After an oxygen exposure of 3 L, upon the formation of a  $c(2 \times 2)$  superstructure on the surface, the spectrum shows remarkable changes. The Co minority peak at 0.9-eV binding energy is slightly suppressed, while its shape and position remain constant. The structure in the majority-spin spectrum changes more drastically. The peak close to  $E_F$  is reduced more than the  $\Delta_5(\uparrow)$  emission at 2.4-eV binding energy, so that this feature becomes more pronounced than in the clean spectrum. This is again evidence for the interpretation of the surface nature of the majority-spin peak near the Fermi energy.

At about 5.8-eV binding energy we observe an oxygen-induced peak that corresponds to the first oxidation phase as discussed above. For symmetry reasons this peak corresponds to the emission from the  $O 2p_{x,y}$  orbitals and it grows in both spin channels. In Fig. 6 the region of this peak is shown enlarged after subtraction of a polarized background. The intensity of this peak is nearly equal in both spin directions, but it shows an exchange splitting of  $(0.2 \pm 0.1)$  eV. The maximum of the majority-spin peak is observed at 5.9 eV and the maximum of the minority-spin peak is located at 5.7-eV binding energy. Since the majority-spin components of the adsorbate-induced features are at higher binding energy than the minority-spin components, it may be deduced that the adsorbate carries a magnetic moment and that this moment is ferromagnetically aligned with the bulk moment of the substrate. This has also been observed for oxygen adsorbed on Fe(001),<sup>5</sup> for which theory predicted an induced magnetic moment at the oxygen sites.<sup>6</sup>

The exchange splitting of the photoemission peaks indicates the presence of a magnetic moment on the adsorbate. However, from this exchange splitting we cannot quantitatively derive the magnitude of that moment. Nevertheless, we can conclude from the induced exchange splitting in the adsorbate site that the topmost Co layers also carry a magnetic moment, i.e., there are no magnetically "dead layers" on the Co surface induced by the adsorbate.

The spectrum in Fig. 5 for 7 L oxygen exposure already shows the transition from the first [ $O-c(2 \times 2)$  reconstruction] to the second (surface-oxide formation) reaction phase. The oxygen-induced emission is much broader than in the 3 L spectrum and an exchange splitting is no longer observable. The minority-spin  $\Delta_5$  peak near the Fermi energy is still clearly visible but its intensity is even more suppressed, while the majority-spin feature near  $E_F$  has changed its shape more drastically. From the surface peak there is now only a shoulder left and one can see the formation of an additional feature around 2-eV binding energy.

The spectrum after 10 L oxygen exposure is again different. Its shape has nearly the form of the oxygen-saturated spectrum; that means this spectrum corresponds mostly to the second reaction phase. One can clearly identify the peaks at 1.9- and 3.8-eV binding energy due to the Co  $3d$  emission of the oxide, the broad structure around 6-eV binding energy which includes the oxygen  $2p$  emission, and the onset of the 10-eV satellite.

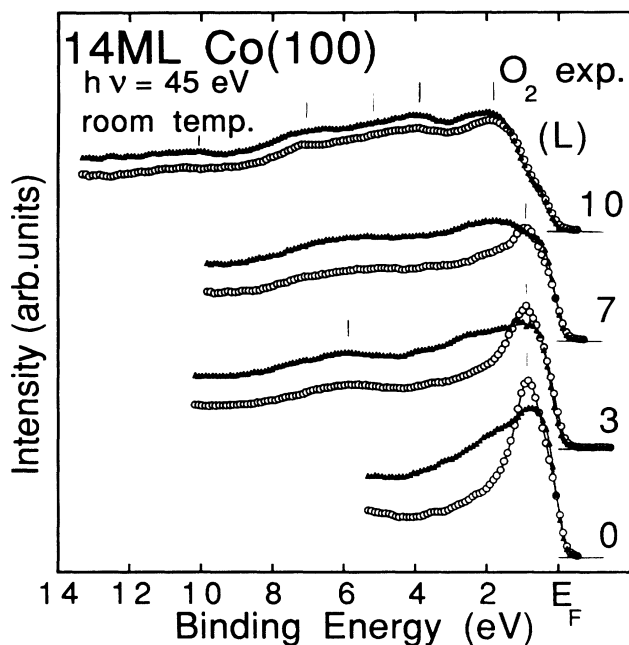


FIG. 5. Spin-resolved photoemission spectra of (14 ML Co)/Cu(100) taken in normal emission with  $s$ -polarized light of 45-eV photon energy. The spectra for different oxygen exposures at room temperature are shown. The filled triangles ( $\blacktriangle$ ) correspond to the emission from the majority electron spin direction and the open circles ( $\circ$ ) to the minority electron spin direction.

All these peaks are visible in both spin channels; there is only a nearly constant small polarization left, due to inelastically scattered electrons from the deeper Co layers. Because the peaks are observed in both spin channels with nearly the same intensity and at the same bind-

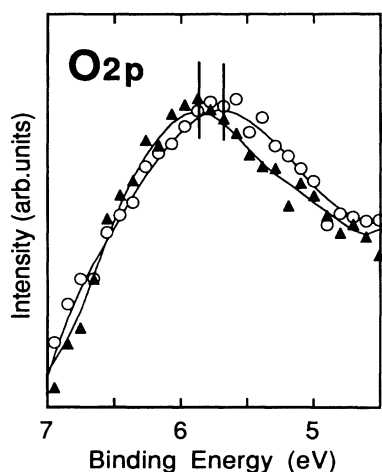


FIG. 6. Spin-resolved spectra of (14 ML Co)/Cu(100) after 3 L oxygen exposure at room temperature in the region of the oxygen  $2p$  emission. A constant polarized background is subtracted. The filled triangles ( $\blacktriangle$ ) correspond to the emission from majority electron spin direction and the open circles ( $\circ$ ) to the minority electron spin direction. The  $2p$  peaks show an induced exchange splitting of  $0.2 \pm 0.1$  eV.

ing energy, we conclude that the surface of the oxidized sample is no longer ferromagnetically ordered. This is not surprising, because CoO is antiferromagnetic with a Néel temperature of about 293 K, only a little below room temperature (298 K). Thus, the oxide might even be in the paramagnetic phase already. We cannot distinguish from our spectra between antiferromagnetic and paramagnetic phases.

The spin-resolved photoemission spectra of the oxidation reaction at low temperature (150 K) (not shown here) exhibit similar behavior to that at room temperature. The spectrum of the clean sample is identical to that at room temperature. But the changes in the spectra occur at lower oxygen exposures compared with the room-temperature reaction, indicating a larger sticking coefficient. After 5 L oxygen exposure the reaction at low temperatures is already in the region between the first and the second reaction phase and the spin polarization is nearly lost. With higher oxygen exposure the polarization in the spectra is totally lost, as expected for the oxide phase.

### C. Core-level spectroscopy

Further support for the distinction we have made between the two reaction stages is derived from the Co  $3p$  core-level spectra. Also, the  $3p$  spectra (Fig. 7) display as a function of oxygen exposure two distinct behaviors. Up to 6 L only small changes can be observed in the  $3p$  line shape, as it is expected for Co weakly interacting with the surface adsorbed oxygen. Above 7 L a 1.5-eV chemically shifted component emerges, corresponding to the formation of surface CoO. The value of the chemical shift is in agreement with published data for CoO.<sup>22</sup>

We have also taken spin-resolved photoemission spectra of the Co  $3p$  core levels. The influence of adsorbates on the spin-dependent electronic structure of core levels has previously been investigated only for the Fe  $3p$  level with oxygen chemisorption.<sup>23</sup> In Fig. 8 we report the spin-resolved spectra of the Co  $3p$  state of the clean sample and after 4 and 12 L oxygen exposure at room temperature. The spectrum of the clean sample is similar to that reported by Kachel *et al.*<sup>24</sup> This spectrum shows an overall dominating majority-spin emission due to the polarization of the background. Only at the Co  $3p$  peak does the minority-spin emission dominate. This polarization dependence at the  $3p$  peak reflects the spin-dependent interaction of the final-state core hole with the net spin of the valence electrons and is similar to that of Fe.<sup>23,25</sup> The Co  $3p$  peak is split by  $0.3 \pm 0.15$  eV. After 4-L oxygen exposure, which corresponds to the first reaction stage, the peaks become broader, but their shapes remain mainly the same. Additional structures appear at about 60-eV binding energy; within the statistical error, the changes in the spectra are identical in both spin channels.

The spectra for 12 L oxygen exposure already show the feature for the second reaction stage. They have nearly the same structure in both spin channels, except that the majority-spin spectrum is still higher in intensity due to background polarization of unreacted Co layers underneath. This is similar to what we have observed in the

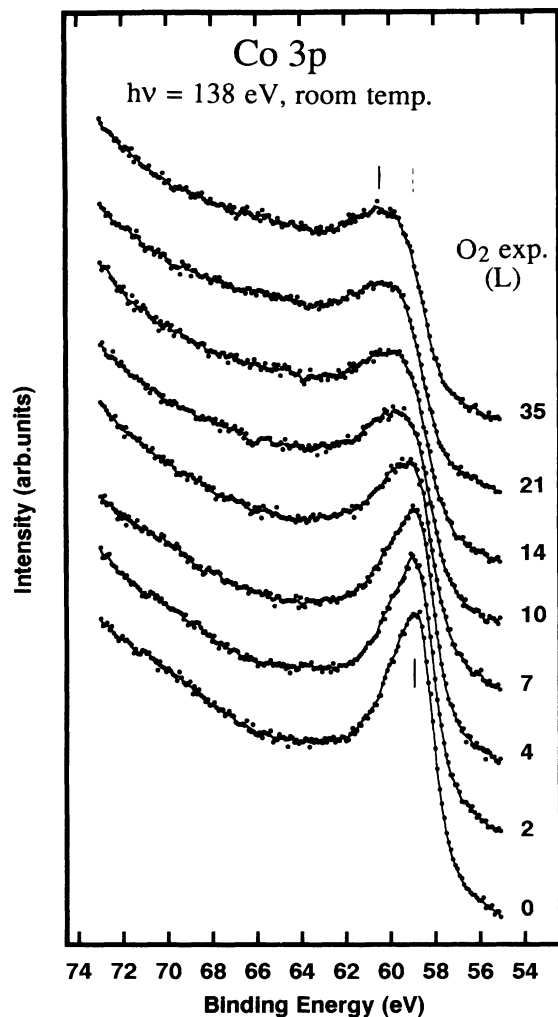


FIG. 7. Spin-integrated photoemission spectra of Co 3p core levels taken at 138-eV photon energy for different oxygen exposures at room temperature. A constant background is subtracted in each spectrum.

spin-resolved valence-band spectra. The additional emission between 60- and 68-eV binding energy is not polarized; it appears simultaneously in both spin channels. This shows again that the surface oxide no longer has long-range ferromagnetic order. This result is different from that which Sinkovic *et al.*<sup>23</sup> have observed for oxidation of the Fe(100) surface. They find in a spin-polarized photoemission study of the initial oxidation of Fe(100) spin-dependent changes in the Fe 3p spectra and deduce the presence of a mostly ferrimagnetic oxide with some contribution from an antiferromagnetic phase.

#### IV. CONCLUSION

Using spin- and angle-resolved photoemission, we found that the reaction of oxygen with the Co(100) surface takes place in two distinct stages. In the first stage, for low-oxygen exposures, the adsorbed oxygen forms a  $c(2 \times 2)$  superstructure on the surface. In this stage the

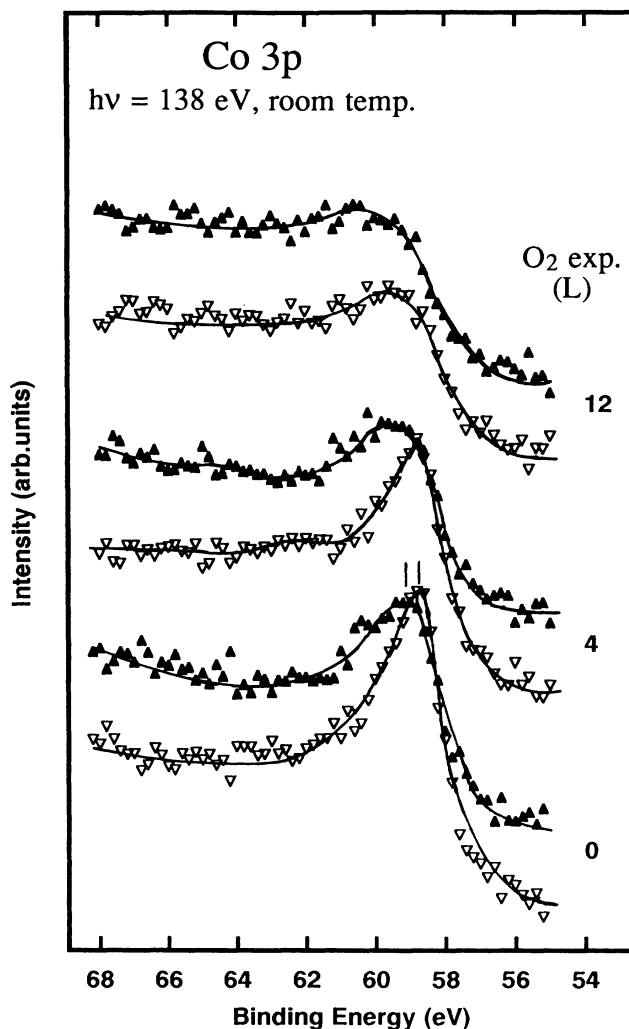


FIG. 8. Spin-resolved photoemission spectra of the Co 3p core levels taken at 138-eV photon energy. The spectra for different oxygen exposures at room temperature are shown. A constant background is subtracted in each spectrum. The filled triangles (▲) correspond to the majority-spin electrons and the open triangles (▽) to the minority-spin electrons.

O-2p-derived bands exhibit an induced exchange splitting of  $0.2 \pm 0.1$  eV. This is proof that there are no magnetically dead layers on the Co surface due to the oxygen adsorption, and is also an indication of the presence of a magnetic moment in the adsorbed oxygen. For higher exposures, the oxygen forms a surface oxide. In this second reaction stage, the long-range surface order is lost and the spin polarization of the photoelectrons vanishes. This is in agreement with the assignment of the formation of CoO at room temperature, and mainly  $\text{Co}_3\text{O}_4$  at low temperatures, which are both antiferromagnets.

#### ACKNOWLEDGMENTS

These experiments were carried out at BESSY. We would like to thank D. Hoffmann (KFA) and the BESSY staff for their valuable technical assistance.

- <sup>1</sup>For a review, see, e.g., L. M. Falicov, D. T. Pierce, S. D. Bader, R. Gronsky, K. B. Hathaway, H. J. Hopster, D. N. Lambeth, S. S. P. Parkin, G. Prinz, M. Salamon, I. K. Schuller, and R. H. Victora, *J. Mater. Res.* **5**, 1299 (1990).
- <sup>2</sup>Peter D. Johnson, *J. Electron Spectrosc. Relat. Phenom.* **51**, 249 (1990).
- <sup>3</sup>G. Schönhense, M. Donath, U. Kolac, and V. Dose, *Surf. Sci.* **206**, 1888 (1988).
- <sup>4</sup>G. Schönhense, M. Getzlaff, C. Westphal, B. Heidemann, and J. Bansmann, *J. Phys. (Paris) Colloq.* **49**, C8-1643 (1988).
- <sup>5</sup>P. D. Johnson, A. Clarke, N. B. Brookes, S. L. Hulbert, B. Sinkovic, and N. V. Smith, *Phys. Rev. Lett.* **61**, 2257 (1988).
- <sup>6</sup>H. Huang and J. Hermanson, *Phys. Rev. B* **32**, 6312 (1985).
- <sup>7</sup>R. G. Musket, W. McLean, C. A. Colmenares, D. M. Makowiecki, and W. J. Siekhaus, *Appl. Surf. Sci.* **10**, 143 (1982).
- <sup>8</sup>C. R. Castro and J. Küppers, *Surf. Sci.* **123**, 456 (1982).
- <sup>9</sup>T. Matsuyama and A. Ignatiev, *Surf. Sci.* **102**, 18 (1981).
- <sup>10</sup>M. Maglietta, E. Zanazzi, U. Bardi, F. Jona, D. W. Jepsen, and P. M. Marcus, *Surf. Sci.* **77**, 101 (1978).
- <sup>11</sup>See, e.g., W. Oed, H. Lindner, U. Starke, K. Heinz, K. Müller, and J. B. Pendry, *Surf. Sci.* **224**, 179 (1989).
- <sup>12</sup>L. Gonzales, R. Miranda, M. Salmeron, J. A. Verges, and F. Yndurain, *Phys. Rev. B* **24**, 3245 (1981).
- <sup>13</sup>A. Clarke, G. Jennigs, R. F. Willis, P. J. Rous, and J. B. Pendry, *Surf. Sci.* **187**, 327 (1987).
- <sup>14</sup>R. Germar, W. Dürr, J. W. Krewer, D. Pescia, and W. Gudat, *Appl. Phys. A* **47**, 393 (1988).
- <sup>15</sup>J. J. de Miguel, A. Cebollada, J. M. Gallego, S. Ferrer, R. Miranda, C. M. Schneider, P. Bressler, J. Garbe, K. Bethke, and J. Kirschner, *Surf. Sci.* **211**, 732 (1989).
- <sup>16</sup>H. Li and B. P. Tonner, *Surf. Sci.* **237**, 141 (1990).
- <sup>17</sup>E. Kisker and C. Carbone (unpublished).
- <sup>18</sup>W. Peatman, C. Carbone, W. Gudat, W. Heinen, P. Kuske, J. Pflüger, F. Schäfer, and T. Schroeter, *Rev. Sci. Instrum.* **60**, 1445 (1989).
- <sup>19</sup>W. Clemens, T. Kachel, E. Vescovo, S. Blügel, C. Carbone, and W. Eberhardt, *Solid State Commun.* **81**, 739 (1992).
- <sup>20</sup>Y. Jugnet and T. M. Duc, *J. Phys. Chem. Solids* **40**, 29 (1979).
- <sup>21</sup>J. van Elp, J. L. Wieland, H. Eskes, P. Kuiper, G. A. Sawatzky, F. M. F. de Groot, and T. S. Turner, *Phys. Rev. B* **44**, 6090 (1991).
- <sup>22</sup>C. R. Brundle, T. J. Chuang, and D. W. Rice, *Surf. Sci.* **60**, 286 (1976).
- <sup>23</sup>B. Sinkovic, P. D. Johnson, N. B. Brookes, A. Clarke, and N. V. Smith, *Phys. Rev. Lett.* **65**, 1647 (1990).
- <sup>24</sup>T. Kachel, C. Carbone, W. Heinen, and W. Gudat (unpublished).
- <sup>25</sup>C. Carbone and E. Kisker, *Solid State Commun.* **65**, 1107 (1988).